geosciences

MDPI

Article

The Lambousa (Cyprus) Fishtank in a Quasi-Stable Coastal Area of the Eastern Mediterranean, a Notable Marker for Testing GIA Models

Fabrizio Antonioli [1,*], Stefano Furlani [2], Giorgio Spada [3], Daniele Melini [4] and Zomenia Zomeni [5]

[1] Institute of Environmental Geology and Geoengineering (IGAG), National Research Council (CNR), 09123 Cagliari, Italy
[2] Department of Mathematics and Geosciences, University of Trieste, 34127 Trieste, Italy; sfurlani@units.it
[3] Dipartimento di Fisica e Astronomia "Augusto Righi", Alma Mater Studiorum Università di Bologna, 40126 Bologna, Italy; giorgio.spada@unibo.it
[4] Istituto Nazionale di Geofisica e Vulcanologia, 00143 Roma, Italy; daniele.melini@ingv.it
[5] Cyprus Geological Survey, Nicosia 1301, Cyprus; zzomeni@gsd.moa.gov.cy
* Correspondence: fabrizio.antonioli@igag.cnr.it

Abstract: The Lambousa fishtank, an archaeological structure entirely carved in bedrock, can be easily recognized and measured in the plan on Google Earth (GE). We surveyed in situ this excellent archaeological marker in 2016 through direct measurements using traditional field instruments, such as metric tapes and invar rods, and terrestrial photogrammetry using Structure from Motion (SfM) methods. The bedrock on which the fishtank is founded is an Upper Pleistocene calcarenite also containing *Persistrombus latus*. The age of the studied fishtank has not been previously published, but on the basis of the construction technique and the interpretation provided by Archaelogist and references therein, we believe that it was built in the period between 2.1 and 1.8 ka BP, like similar fishtanks in the Mediterranean area. Architectural structures consist of evident foot walks (*Crepido*), a stone base, and a tunnel that allows for seawater exchange during high tides. The tunnel is at the same altitude as the *Crepido*, which lies around the fishtank. These architectural components allow us to evaluate the palaeo-sea level with significant precision during the time when the fishtank was active. MIS 5.5 coastal deposits that outcrop in the study area are located at a maximum altitude of a few meters, while the inner margin of the MIS 5.5 terrace allows us to hypothesize "quasi-tectonic stability". We have also obtained several predictions of the contribution from Glacial Isostatic Adjustment (GIA) to relative sea level at Lambousa for the past 3.5 kyr, according to models ICE-6G (VM5a), ICE-7G (VM7), and one of the GIA models by the Australian National University ANU) Research group.

Keywords: fishtanks; GIA; relative sea level; MIS 5.5 highstand; Cyprus; Mediterranean Sea

Citation: Antonioli, F.; Furlani, S.; Spada, G.; Melini, D.; Zomeni, Z. The Lambousa (Cyprus) Fishtank in a Quasi-Stable Coastal Area of the Eastern Mediterranean, a Notable Marker for Testing GIA Models. *Geosciences* **2023**, *13*, 280. https://doi.org/10.3390/geosciences13090280

Academic Editors: Markes E. Johnson and Jesus Martinez-Frias

Received: 8 June 2023
Revised: 4 September 2023
Accepted: 10 September 2023
Published: 14 September 2023

1. Introduction and State of the Art

The aim of this research is to evaluate the relative sea-level changes at the site of the Lambousa fishtank (***ft***), first reported by Galili et al. [1] on the northern coast of Cyprus, at the time slice between today and 2 ka BP. The authors did not evaluate sea level changes, while here we use it, just as a very precise sea level marker, as suggested by [2]. Roman ***fts*** were built mainly along the Mediterranean coast [3–8], and they followed precise construction rules. The architectural elements of the Mediterranean ***fts*** are: the channels, the sluicegates, and the foot walk, also named *Crepido*, which, if well-preserved, bears directly on mean sea level at the time of construction and provides a precise measurement of the relative sea level change from the time of construction. Mediterranean ***fts*** were built in a short time interval between 2.1 and 1.9 ka BP [5]. The archaeological interpretation must initially establish the maritime and/or nature and vocation of the site (harbor, fishtanks,

etc.), determine its typology and specific usage, analyze the elements of its building techniques (that reveal themselves as meaningful markers of height or depth at the time of building) and its functional elements, such as the height of the emerged part with respect to the mean sea level, and point out the time of construction and its chronological range of usage and frequentation. The evaluation of both the height and functional depth to the mean sea level depends on the typology of the archaeological evidence, its use, and the local tide amplitudes [2]. For example, the surface of a pier surely has a functional elevation different from that of a haulage area, a quarry, or a pavement. The functional height of a pier and its relationship with the current and past sea level depends on the size and height of the hull of the ship using the dock. The functional height of a ***ft***, if measured at *Crepido* connected with a sluicegate, is assumed to be zero. The palaeo sea level of a ***ft*** is instead the measure between *Crepido* and the present sea level and must be corrected for the local tide and pressure [2,5].

2. Study Area

The study site is located on the rocky coast of Karavas village, 10 km west of the city of Keryneia. Flinder [9] mentioned it as a Lapithos fishtank. He described the tank, and the channels, and assumed that the channels were provided double sluicegates (absent today), but he did not describe the tunnel we found in the northern portion of the Lambousa ***ft***, probably because it was covered by sand. Then Flinders observed that a wall placed to the north, at the tunnel, was repaired and thus protected the ***ft*** from the waves [9]. At the end, Flinder observed a maximum of 12 cm of tide in 24 h and described the lateral channels as a supplementary exchange of water in some unfavorable wind conditions. He compared this ***ft*** to those described by [3] in Torre Valdaliga (Italy) and wrote:

> *"Lapithos (Lambousa) remained an important city into Graeco-Roman times for we know from Ptolemy, the geographer that in the middle of the second century AD, Lapithos was one of the four districts of Cyprus, the others being Salamis, Paphos, and Amathus. Again, a principal oblong tank of similar proportion contains feeder channels, straddled by secondary tanks, slotted sluice gates, and smaller tanks unconnected to the main tank. Both sites also possess similar traditional names: Caesarea, The Pool of Cleopatra, and Lapithos, The Pool of the Queen."*

Indirectly, therefore, Flinders restricted the chronological attribution to the Roman Age. In the Greek Age, there were no known ***fts***. In particular, all the Tyrrhenian ***fts*** (most of those studied) date between the first century BC and the first century AD [5,6].

The ***ft*** we studied is carved in a Quaternary marine deposit consisting of a well-cemented and fossiliferous calcarenite, which we attribute to Marine Isotope Stage MIS 5.5 because we find at about 150 m from the Lambousa ***ft*** the MIS 5.5 transgression (calcarenite) at about 1 meter from the present sea level. From a geological point of view, Cyprus, the third-largest Mediterranean island, is notable for its geodiversity and tectonics, both of which have created a unique landscape and natural environment (Figure 1). [10] could not have made a more representative statement about the geology of Cyprus and its ophiolite when stating that *"one of the most fascinating aspects of eastern Mediterranean geology is the very rapid Plio—Quaternary uplift of the Troodos ophiolite"*. The age of the rock outcropping on the northern part of Cyprus span from the Permian to the present. Four distinct geological terraces are partly covered by surficial sediments. These lands, their lithologies, and their tectonic history contribute to the saping of the island.

The tectonic setting of Cyprus is commonly considered to be that of a compressional zone between the northward-moving African Plate and the westward-moving Eurasian Plate, a tectonic compression that is bound to close the eastern Mediterranean in the geological future. Recent earthquakes show left transpressional motions along the Cyprus arc off SW Cyprus and the Florence Rise, while extensional earthquakes are abundant in the region of southern Anatolia off Cyprus [10], Figure 2.

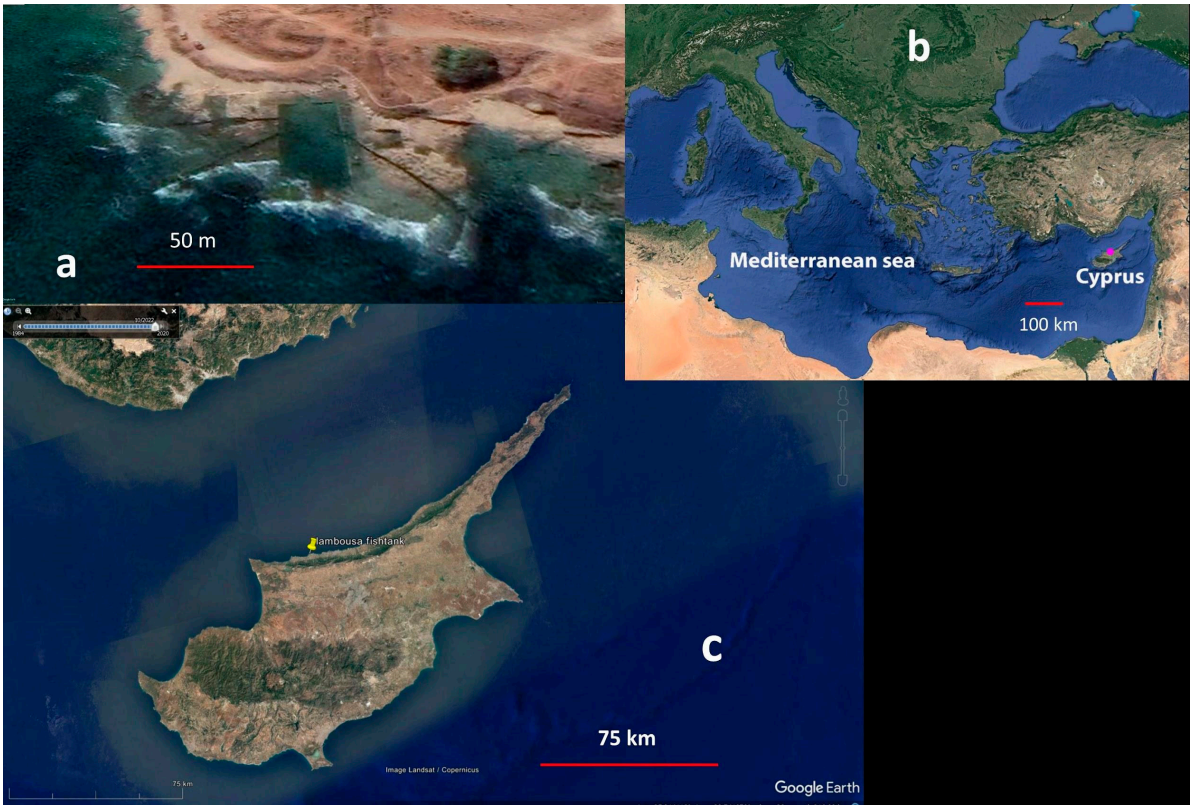

Figure 1. (**a**) the Lambousa *ft* located on the northern coast of Cyprus (**b**) Mediterranean Sea and Cyprus, (**c**) Cyprus and the *ft* position.

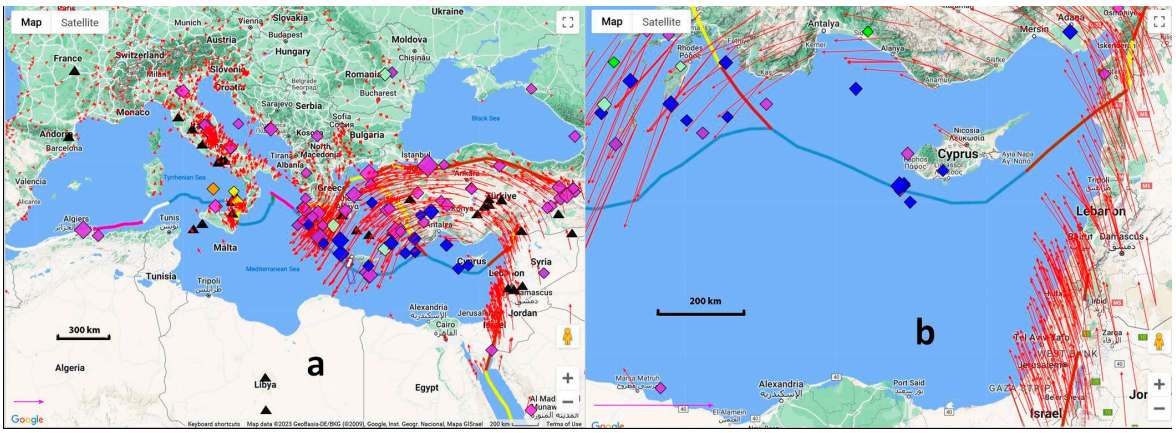

Figure 2. From UNAVCO. GPS velocity (red arrows) vector plate boundary (colored thick lines), volcanoes (black triangles), earthquakes (colored polygons). (**a**) the Mediterranean map, (**b**) a detailed view of Cyprus. For a precise legend, see: https://www.unavco.org/software/visualization/GPS-Velocity-Viewer/GPS-Velocity-Viewer.html. Accessed on 15 June 2023.

Regarding the Late Pleistocene tectonics, in her Ph.D. thesis [11], she has studied numerous coastal sites in Cyprus where flights of marine terraces range in age from MIS 5.3 to MIS 17. Archiving older work and using new analyses/dating of different methods (Radiocarbon, U/Th, Osl, Ar/Ar, cosmogenic) a total of 21 samples in 14 different coastal sites provide evidence for the uplift rates of MIS 5.5, including the site where the Lambousa *ft* is located. Moreover, Zomeni also published figures on the Cyprus terraces, in particular all those concerning the MIS 5.5 transgression. Regarding the Late Pleistocene tectonics, Figures 2–7 of [11] show the vertical distribution of marine terraces in 17 different coastal sectors around the island. The marine terraces' inner margins related to the MIS 5.5

transgression are found at elevations between +1.8 and +32 m above present sea level. These terraces have been dated with ESR or U/Th; these datings have been confirmed in MIS 5.5 also for the presence of *Persistrombus latus* or other Senegalese fauna. For a large area of the north coast of Cyprus (where the Lambousa ***ft*** is located), [11] provides an uplift rate of 0.12 mm/year. [1] studied 22 MIS 5.5 sections, including a site (site number 9) at Lambousa. By combining already published dating results with several new observations and analyses, he provided the uplift rate (mm/year) for the terraces. In Figure 3, we combine these observations with those of [1] for the coastal area of the Lambousa ***ft***.

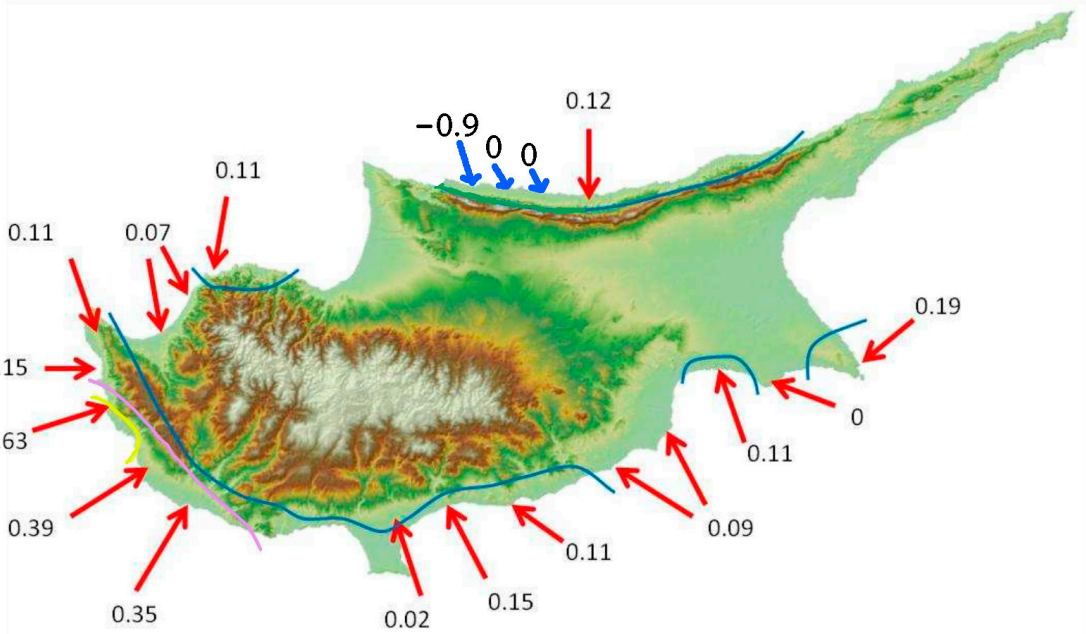

Figure 3. Vertical tectonics rates on the coast of Cyprus from the Last Interglacial (118 kyr). Rates marked with a red arrow are from [11] while those marked with a blue arrow are from [1]. All rates are in units of mm/yr. The blue, purple, and yellow lines mark the 0.1, 0.2, and 0.4 mm/year uplift isolines, respectively. From [11].

3. Materials and Methods

Sea-level change along the Mediterranean coast is the sum of eustatic (ice melt), glacio-hydro-isostatic (GIA), and tectonic factors. The first contribution is globally uniform and time-dependent, while the latter two also vary with location. The glacio-hydro-isostatic part exhibits a well-defined pattern and is readily predictable once the spatiotemporal evolution of ice sheets and the Earth rheological structure are defined; estimates of present-day rates of sea level change due to GIA in the Mediterranean are well below the 1 mm/year level [11]. Conversely, the tectonic component must be estimated for each site, with present-day rates in the Mediterranean varying between +2 and −2 mm/year [12]. Together, these components result in a complex spatial and temporal pattern of relative sea level change around the Mediterranean coastline [5].

3.1. Surveys

The survey of the Lambousa ***ft*** was carried out using a metric rod to measure the size of the entry hole (the tunnel located at the northern part of the ***ft*** that connects the ft with the outside) and to measure the *Crepido*. The sea level altitudes were corrected for the tide using predictions from the Xtide site (https://flaterco.com/xtide/files.html#xtide, see Figure 4). The atmospheric pressure during the measurements on-site was 1016 bar; therefore, no sea level correction for pressure has been made.

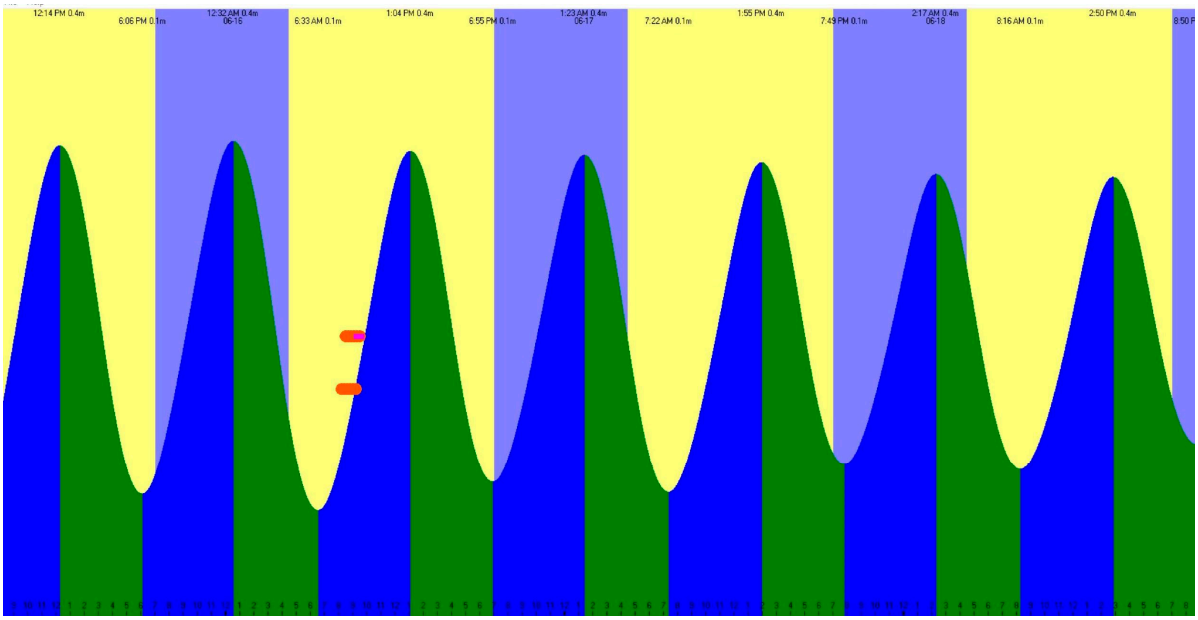

Figure 4. Tide variation during the survey of 06.06.2016 on the *Crepido* (09.15 A.M.) and on the Tunnel (09.45 A.M.). The tide varied from +18 to +22 cm. Red lines indicate the timing of in situ measurement. The plot is from the Xtide website (https://flaterco.com/xtide/files.html#xtide). Accessed on 4 April 2023.

3.2. GIA

Glacial Isostatic Adjustment (GIA) is the still ongoing response of the Earth system to spatiotemporal variations of surface loads during the last glacial cycle. GIA is a global process contributing to present and past vertical land deformation, variations of the gravity field, and sea level change. As discussed by [13], in regions located in the far field of the former ice sheets, such as the Mediterranean basin, GIA is mostly acting through lithospheric flexure in response to the hydro-isostatic effect of meltwater load. A quantitative description of GIA is provided by the Sea Level Equation (SLE), first introduced by [13], which in its simplest form reads:

$$S(\phi, \lambda, t) = N(\phi, \lambda, t) - U(\phi, \lambda, t)$$

where S, N, and U represent sea level change, sea surface variation, and vertical land displacement at time t on a point of latitude ϕ and longitude λ, respectively. As discussed by e.g., [14], N and U depend also on S through spatiotemporal convolutions, making the SLE an integral equation that shall be solved numerically by means of iterative methods. To reconstruct the history of relative sea level at the site of Lambousa, we obtained a numerical solution of the SLE with solver SELEN4 [14]. SELEN4 solves the SLE above through the pseudospectral approach, assuming a laterally homogeneous, spherical, incompressible, and self-gravitating Earth characterized by a Maxwell rheological law. The SLE accounts for horizontal migration of shorelines (see e.g., [15,16]) and for the effects of rotational feedback on sea level, according to the revised rotational theory proposed by [17].

To obtain a numerical solution to the SLE, the spatiotermporal evolution of the former ice sheets as well as the rheological profile of the Earth shall be defined a priori. To estimate predictions of past sea level at the Lambousa site, we integrated into SELEN4 the GIA models ICE-6G (VM5a) of [18,19], ICE-7G (VM7) of [20,21], and one of the models progressively developed by the Australian National University (ANU) by Kurt Lambeck and collaborators (see e.g., [22]). Since the Mediterranean basin is characterized by a complex geodynamic setting whose rheological structure is likely to significantly depart from the globally averaged 1D profiles employed in GIA models, it is important to estimate the sensitivity of GIA predictions to possible variations of the rheological model [23,24].

To this aim, we evaluated the uncertainties associated with GIA predictions from ICE-6G and ICE-7G by generating two random ensembles of 10,000 GIA models based on perturbations of the VM5a and VM7 viscosity profiles, while for the ANU, we considered the mini-ensemble of 7 GIA models employed by [22] for the Mediterranean basin.

4. Data

4.1. Field Data

We obtained new data with simple observations, photographs, and measurements using a meter stick, of some archaeological markers on the ***ft*** (see Figures 5 and 6). In particular, we found a *Crepido* at −0.44 m from sea level at the time of measurement and an exit inlet hole (a tunnel on the northern portion of the ft) between −0.44 and −1.0 m (Figure 6b–d).

Figure 5. The Lambousa ***ft***. See also Figure 1a.

We measured the *Crepido* (Figures 7–9) at 9.15 A.M. in the morning, which was at −0.44 m from sea level, showing dimensions similar to the same archaeological markers studied and measured in many Mediterranean fishtanks [5]. The ***ft*** bottom, certainly deeper than 2 m, is today filled with stones and sand. In the long lateral channels (Figures 6a and 7), as also described by [9], it is possible to note sluicegates, which regulated the flow of the water and presumably prevented the fish from escaping. We found one of the most interesting points on the northern portion of the ***ft*** where a tunnel about 2 m long has a minimum width towards the outside of about 50 cm and can be seen both inside and outside of the ft (the dimensions are: the base at −1.0 m and the roof at −0.44 m from sea level at the time of measurement). This tunnel currently works as a replacement, and while the long external canals are silted up and partly filled with stone, they are no longer functional.

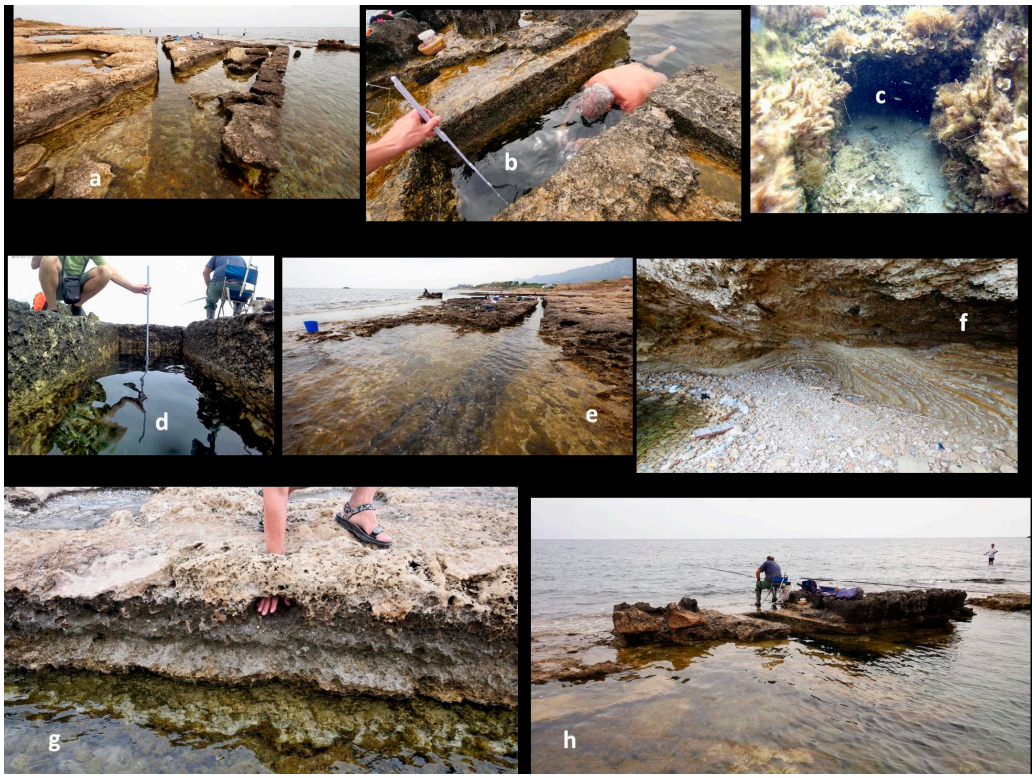

Figure 6. Image collection of the Lambousa *ft* with descriptions of some archaeological markers. (**a**) external channels; (**b**–**d**) the tunnel with a submerged channel with the connection with the sea; (**e**) a second external channel; (**f**) the transgression of the MIS 5.5 calcarenite on which the *ft* was carved and the bedrock; (**g**) an artificial hole; (**h**) the tunnel and submerged channel observed from a different perspective.

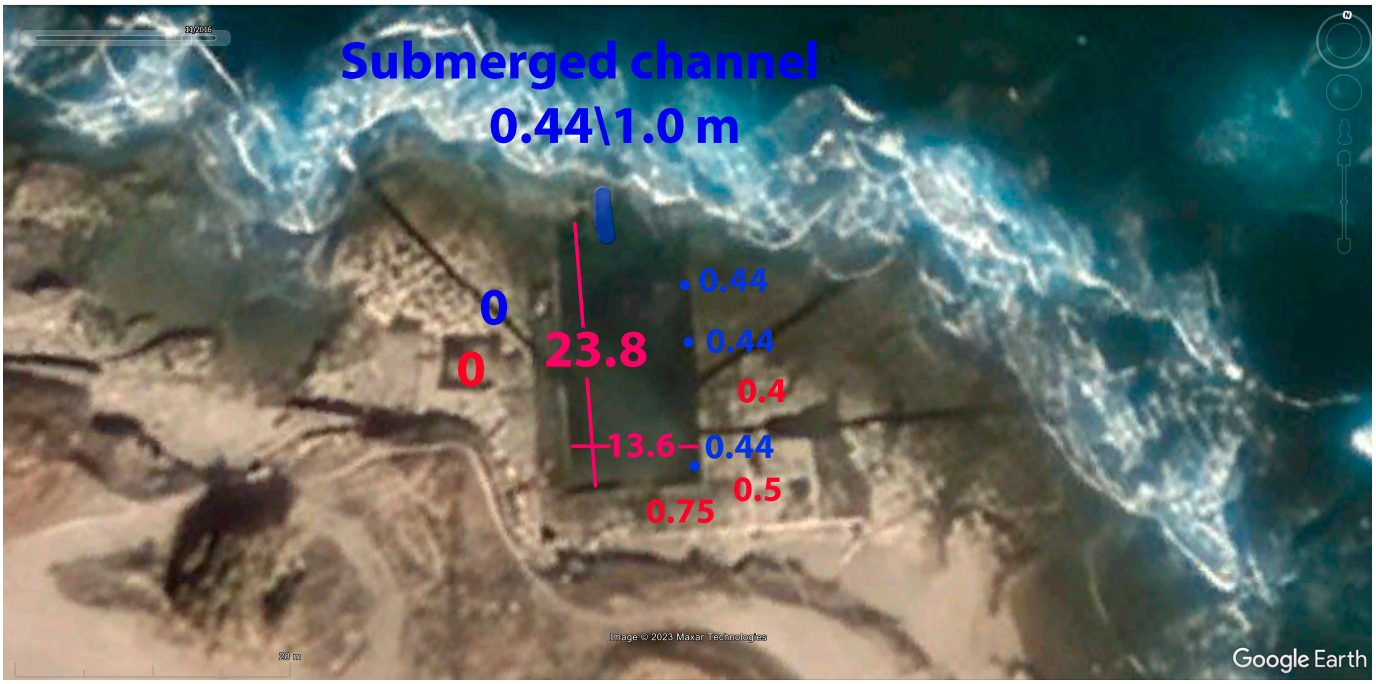

Figure 7. The Lambousa fishtank from Google Earth. The subaerial and underwater observation measurements (in meters) are shown in red (above sea level) and blue (below sea level) respectively.

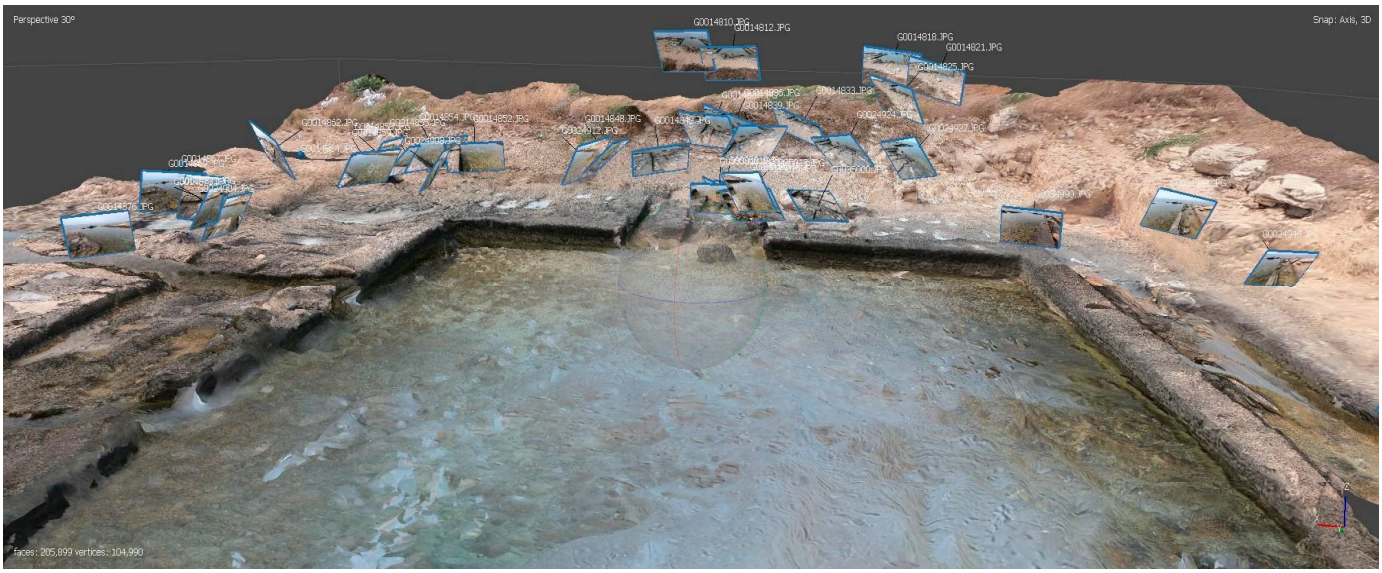

Figure 8. Northern sector of the Lambousa ***ft*** reconstructed with the photogrammetric method. The width of the fishtank is 13.6 m, while the length is 23.8 m (see also Figure 7).

Figure 9. The submerged *Crepido* (highlighted in red) of the Lambousa ***ft*** that we observed, at −0.44 m at the time of the photo.

We corrected for the tide (according to Xtide model, https://flaterco.com/xtide/) our measurements that we made on 16 June 2016. The tide at 09:00 A.M. was 0.18 m, while at 10:30 A.M. was 0.28 m (above zero, Figure 4). Also, we measured the atmospheric pressure with a Casio mod. Protrek digital barometer, the value was 1016 bar, so no corrections for pressure have been applied.

The measurements we carried out on ft at 9.00 A.M. at the *Crepido* and 9:45 A.M. on the tunnel must therefore be corrected and decreased by 0.18 m for the *Crepido* and 0.22 m for the tunnel, and then corrected to −0.26 and −0.78 m, respectively. The mean sea level at about 2 kyr BP of the ***ft*** was therefore to be inferred at an average altitude between these two measurements, i.e., at −0.52 m.

4.2. GIA

In Figure 10, solid lines show predictions for the history of relative sea level at Lambousa for the past 3.5 kyr according to GIA models ICE-6G (VM5a), ICE-7G (VM7), and the GIA model by [22], hereinafter referred to as ANU. All the predictions have been obtained with the SELEN4 SLE solver [14]. For ICE-6G and ICE-7G, shaded regions show the standard deviation of RSL computed over an ensemble of 10,000 GIA models based on random variations of the VM5a and VM7 viscosity profiles, respectively, where the lithospheric thickness and the viscosity profile in the upper mantle have been perturbed with respect to the nominal values. For the ANU GIA model, the shaded region corresponds to the range of RSL obtained with the mini-ensemble of models E1 through E7 as defined in the work of [22]. The differences between the three RSL curves in Figure 10 reflect different assumptions about the ice sheet deglaciation histories and the viscosity profile in the mantle, while the amplitude of the shaded region is a measure of the sensitivity of each GIA model to possible regional variations of rheological parameters.

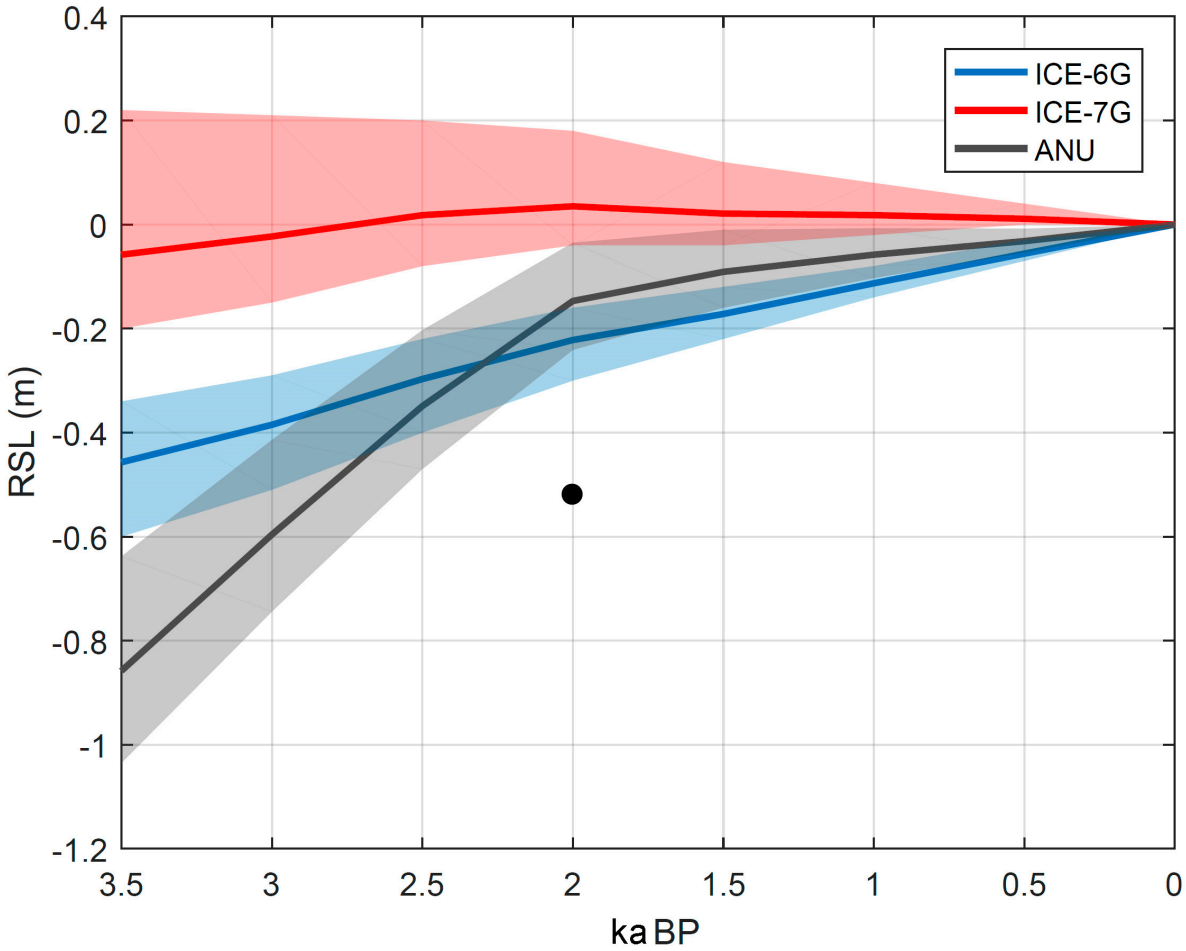

Figure 10. *Relative sea level* change at the Lambousa ***ft*** site during the past 3.5 kyr according to the GIA models ICE-6G (VM5a), ICE-7G (VM7), and one of the GIA models progressively developed by the Australian National University research group (ANU). The shaded regions correspond to the uncertainty level associated with each RSL curve. A black dot marks the relative sea level at Lambousa obtained from our data: −0.52 m.

From Figure 10, we see that our implementation of ICE-7G predicts a substantially stable sea level at Cyprus during the past ~3 kyr, while for ICE-6G and ANU, we obtain an RSL gradually rising to the present level, albeit at different rates. At 2 kyr BP, for ICE-6G and ANU, we obtain a relative sea level of about −0.2 m, with associated uncertainties at the 0.1 m level. For ANU, our result is significantly smaller than the estimate by [22], who

obtained an RSL of about −0.75 m for Cyprus at 2 kyr BP. For ICE-6G (VM5a) and ICE-7G (VM7), [23] estimated an RSL at 2 kyr BP in Cyprus in the range between −0.25 m and −0.50 m; while our estimate for ICE-6G is comparable, considering the uncertainty range, for ICE-7G, we obtain a significantly smaller RSL. Those differences are likely to reflect the structural uncertainties for GIA models, as discussed by [24], and may be attributed to different approaches to the solution of the SLE, including different assumptions about the Earth's compressibility.

5. Discussion

We believe that the vertical movements observed on the northern coast of Cyprus in the ***ft*** coastal area between 2 ka BP and today can be considered null. Even if, as is clearly evident, Cyprus is located in a tectonically active area showing terraced platforms that reach altitudes of up to 400 m [11], we think that no tectonic corrections should be made for the time slice of the last 2 ka.

Instrumental records from GPS or tide gauges longer than 6 years are not available at Lambousa. Observing the time series provided by the Sentinel satellite and published by the European Copernicus site (Figure 11a,b) near Lambousa ***ft***, we see a trend that could indicate slight subsidence; however, on the basis of a recent work [25] which compares long-term geological-archaeological (late Holocene) and instrumental data, we think that the trend of Figure 11b indicates substantial stability for the last 6 years. Indeed, [25] analyzed space geodetic data from the Sentinel-5 satellite released by the Copernicus European Ground Motion Service for the 2016–2021 time range. In this work, the authors have shown some areas where there is a sound consistency between long-term geological data (MIS 5.5 altitude variation) and short-term Sentinel data (e.g., the vertical component of movement in the period 2016–2021). For example, in the Po delta and Venice (NE Italy), the strong correlation is also confirmed by vertical deformation measured by GPS over a period three times that of the interferometric data. In the Pontina Plain (Central Italy), the comparison seems to be well correlated with MIS 5.5 altitude variations. Conversely, in some stable coastal areas of the Mediterranean such as Sardinia or the southern coast of France, where the MIS 5.5 altitude indicates strong vertical tectonic stability [26], the Sentinel data often indicate a very small subsidence, with the same trend detected in Cyprus (Figure 11b).

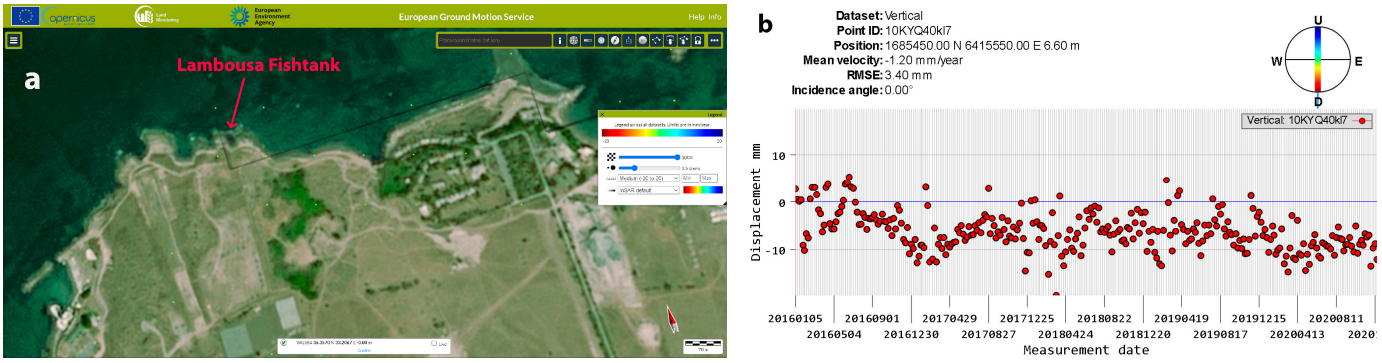

Figure 11. (**a**) Image from Copernicus land monitoring, from the European ground motion service, satellite Sentinel (https://egms.land.copernicus.eu/); (**b**) Time history of vertical displacement at the site marked by a red arrow in Figure 11a, the grashowing substantial stability for the last 6 years.

GIA-driven sea level change in the Mediterranean basin is known to be controlled mostly by lithospheric flexure and hydro-isostatic effects (see, e.g., [15]). The range of GIA models that we considered predict, at 2 ka BP, a minimum relative sea level in Cyprus of about −0.25 m, according to our implementation of the ICE-6G and ANU GIA models, and up to a maximum of −0.75 m, according to [22]. Results from [23] for the ICE-6G (VM5a) and ICE-7G (VM7) GIA models point to an intermediate estimate between −0.25 and −0.50 m.

In our work in order to calculate MIS 5.5 vertical movements we have used the maximum transgression of 7.2 m corrected by GIA and 118 ka as maximum timing [26].

GIA models show that the predicted sea levels at 2 ka BP range between ~−0.25 m and ~0.05 m asl (Figure 9). Ref. [22] obtained a value of ~−0.5 m bsl for the same period. Field data collected at the Lambousa fishtank highlighted a sea level of about −0.52 m. The archaeological structure is built by directly excavating the bedrock, so possible gravitational adjustments of the material composing it are to be ruled out. Considering that the tectonic behavior of the study area suggested by [11] excludes the presence of tectonic movements from the Tyrrhenian onward, ref. [22]'s modified model well fits with field data. However, it is not possible to exclude more recent subsidence subsequent to the use of the ***ft*** that we measured at −0.52 m that could have lowered the structure, e.g., during the Medieval Age, or general tectonic re-adjustments of the area of about 30 cm in the last 2 ka.

6. Conclusions

Data collected at the site of Lambousa allowed us to reconstruct the relative sea level at the time when the fish tank was in use. Previous studies identified several ***fts*** scattered mostly along the coasts of the Central Mediterranean Sea, such as in Crete or Israel (Figure 12). On tectonically stable coasts, the elevation of sea level at the time of the ***fts*** construction varies according to GIA. In the few coastal areas that are undergoing uplift, as in Crete [27], or Briatico (Southern Italy, [28]) or subsidence (such as in the Adriatic area [4]), it is possible to find an elevation difference of as much as 7 m. The Lambousa ***ft***, on the basis of the Flinder interpretation [9], the construction techniques, and our in situ observations, is attributed to an age of 2 ± 0.1 ka. The coastal area of Lambousa has been tectonically stable since the period of construction, a conclusion based both on geological and instrumental markers and, according to our corrected tide and pressure measurements, the mean sea level at 2 ka BP (according to the data of the *Crepido* and the base of the tunnel) was −0.52 m. The GIA models used in this study substantially confirm this measurement.

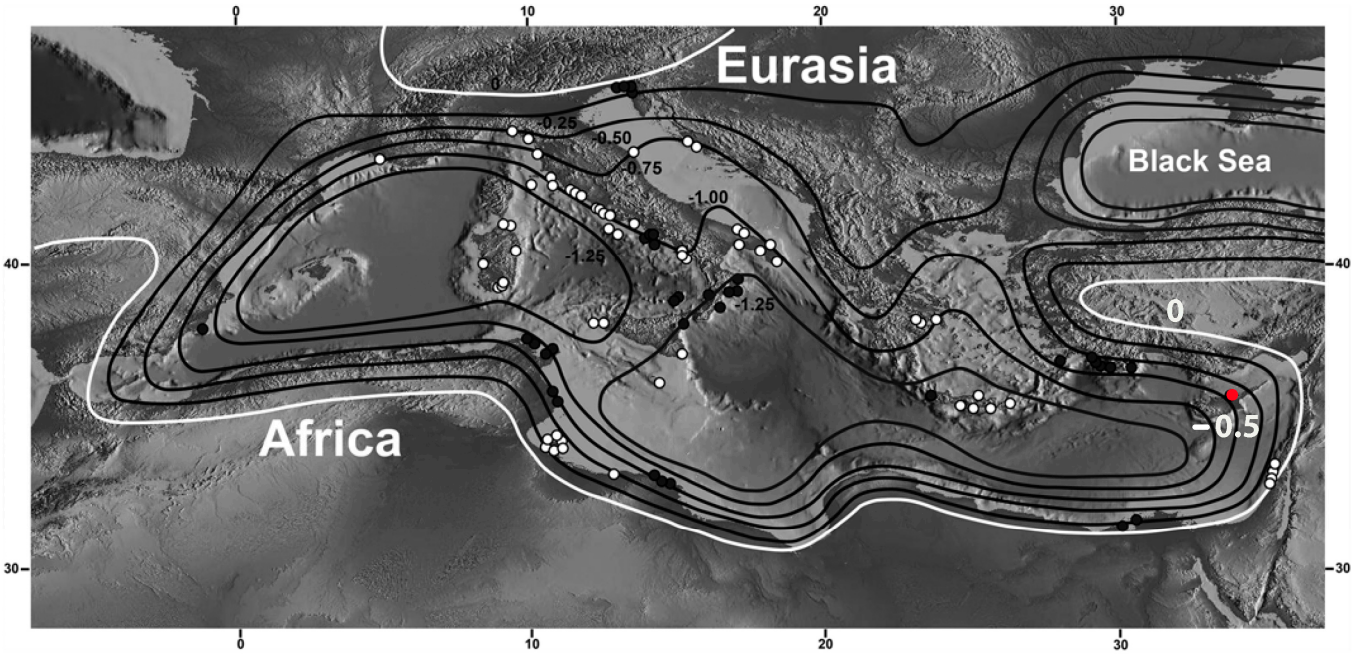

Figure 12. Estimated relative sea levels and shorelines across the Mediterranean at 2 ka BP (modified from [16]). The contour interval is 0.25 m. Black contours are negative values and white contour is zero change. The red dot represents the position of the Lambousa ft pool, between −0.50 and −0.75 m, but closer to −0.50 m.

The difference (between 20 and 30 cm) between the altitude from the geophysical models and the measured infield measurements could be associated either with slight local

subsidence (Figure 11b) or with the fact that the models we considered assume an average 1D global rheological profile, while on a Mediterranean scale, there are marked structural heterogeneities (see, e.g., [29] and references therein), which could potentially amplify the hydro-isostatic effects.

With the measurement of the archaeological marker of Lambousa ***ft***, the calculation of vertical tectonic rates, and the GIA, we have contributed to filling the knowledge gap about the altitude of ***fts*** in the Mediterranean Sea. In fact, in a recent (2022) research paper [30] that published all the studied ***fts*** on the Mediterranean coast, the Lambousa ***ft*** of Cyprus was not reported (Figure 13). Finally, we believe that this new data is very useful to improve the sea level rise models expected in 2100 in the low-lying coastal plains of Cyprus.

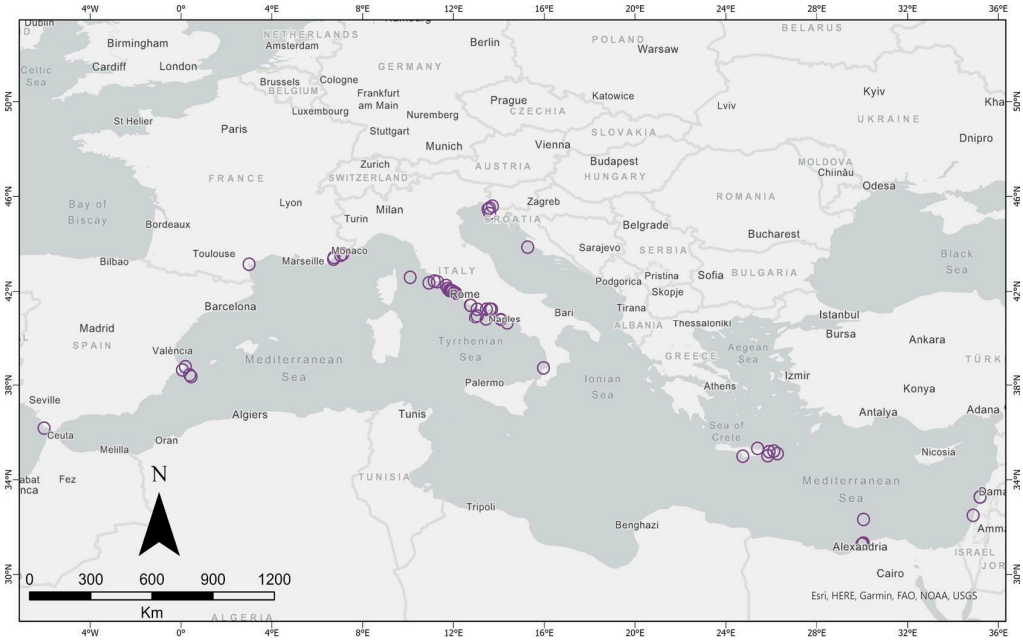

Figure 13. Fish tank distribution (purple dots) across the Mediterranean Sea. Modified from [30].

Author Contributions: Conceptualization, F.A. and S.F.; methodology, S.F., G.S., D.M. and Z.Z.; software, S.F., G.S. and D.M.; validation, F.A., S.F. and Z.Z.; investigation, F.A. and S.F.; data curation, S.F. and D.M.; writing original draft preparation, F.A.; writing review and editing, F.A., S.F., G.S., D.M. and Z.Z.; supervision, S.F. and Z.Z. All authors have read and agreed to the published version of the manuscript.

Funding: This research received no external funding.

Data Availability Statement: Not applicable.

Acknowledgments: We greatly acknowledge two anonymous reviewers who gave us the opportunity to increase the clarity of our manuscript.

Conflicts of Interest: The authors declare no conflict of interest.

References

1. Galili, E.; Sevketoglu, M.; Salamon, A.; Zviely, D.; Mienis, H.K.; Rosen, B.; Moshkovitz, S. Late Quaternary beach deposits and archaeological relicts on the coasts of Cyprus, and the possible implications of sea-level changes and tectonics on the early populations. *Geol. Soc. Lond. Spec. Publ.* **2015**, *411*, 179–218. [CrossRef]
2. Auriemma, R.; Solinas, E. Archaeological remains as sea level change markers: A review. *Quat. Int.* **2009**, *206*, 134–146. [CrossRef]
3. Schmiedt, G. *Il Livello Antico del Mar Tirreno, Testimonianze da Resti Archeologici*; E. Olschki: Firenze, Italy, 1972; 323p.
4. Florido, E.; Auriemma, R.; Faivre, S.; Radi'c Rossi, I.; Antonioli, F.; Furlani, S.; Spada, G. Istrian and Dalmatian fishtanks as sea-level markers. *Quat. Int.* **2011**, *232*, 105–113. [CrossRef]
5. Lambeck, K.; Anzidei, M.; Antonioli, F.; Benini, A.; Esposito, A. Sea level in Roman time in the Central Mediterranean and implications for recent change. *Earth Planet. Sci. Lett.* **2004**, *224*, 563–575. [CrossRef]

6. Lambeck, K.; Anzidei, M.; Antonioli, F.; Benini, A.; Verrubbi, V. Tyrrhenian sea level at 2000 BP: Evidence from Roman age fish tanks and their geological calibration. *Rend. Lincei. Sci. Fis. Nat.* **2018**, *29*, 69–80. [CrossRef]
7. Mourtzas, N. Fish tanks of eastern Crete (Greece) as indicators of the Roman sea level. *J. Archaeol. Sci.* **2012**, *39*, 2392–2408. [CrossRef]
8. Mourtzas, N. Archaeological indicators for sea level change and coastal neotectonics deformation: The submerged Roman fish tanks of the gulf of Matala, Crete, Greece. *J. Archaeol. Sci.* **2012**, *39*, 884–895. [CrossRef]
9. Flinder, A. The fish-tanks. *Int. J. Naut. Archaeol.* **1976**, *5*, 136–141. [CrossRef]
10. Mart, Y.; Ryan, B.F. The complex tectonic regime of the Cyprus Arc: A short review. *Isr. J. Earth Sci.* **2015**, *51*, 117–123. [CrossRef]
11. Zomeni, Z. Quaternary Marine Terraces on Cyprus: Constraints on Uplift and Pedogenesis, and the Geoarchaeology of Palaipafos. Ph.D. Thesis, Oregon State University, Corvallis, OR, USA, 2012.
12. Ferranti, L.; Antonioli, F.; Mauz, B.; Amorosi, A.; Dai Pra, G.; Mastronuzzi, G.; Monaco, C.; Pappalardo, M. Markers of the last interglacial sea-level high stand along the coast of Italy: Tectonic implications. *Quat. Int.* **2006**, *145*, 30–54. [CrossRef]
13. Farrell, W.E.; Clark, J.A. On postglacial sea level. *Geophys. J. R. Astron. Soc.* **1976**, *46*, 647–667. [CrossRef]
14. Spada, G.; Melini, D. SELEN4 (SELEN version 4.0): A Fortran program for solving the gravitationally and topographically self-consistent sea-level equation in glacial isostatic adjustment modeling. *Geosci. Model Dev.* **2019**, *12*, 5055–5075. [CrossRef]
15. Spada, G.; Melini, D. New estimates of ongoing sea level change and land movements caused by Glacial Isostatic Adjustment in the Mediterranean region. *Geophys. J. Int.* **2022**, *229*, 984–998. [CrossRef]
16. Peltier, W.R. Global glacial isostasy and the surface of the ice-age Earth: The ICE-5G (VM2) model and GRACE. *Annu. Rev. Earth Planet. Sci.* **2004**, *32*, 111–149. [CrossRef]
17. Mitrovica, J.X.; Milne, G.A. Glaciation-induced perturbations in the Earth's rotation: A new appraisal. *J. Geophys. Res. Solid Earth* **1998**, *103*, 985–1005. [CrossRef]
18. Argus, D.F.; Peltier, W.R.; Drummond, R.; Moore, A.W. The Antarctica component of postglacial rebound model ICE-6G_C (VM5a) based upon GPS positioning, exposure age dating of ice thicknesses, and relative sea level histories. *Geophys. J. Int.* **1988**, *198*, 537–563. [CrossRef]
19. Peltier, W.R.; Argus, D.F.; Drummond, R. Space geodesy constrains ice-age terminal deglaciation: The global ICE-6G_C (VM5a) model. *J. Geophys. Res. Solid Earth* **2015**, *120*, 450–487. [CrossRef]
20. Roy, K.; Peltier, W.R. Glacial isostatic adjustment, relative sea level history and mantle viscosity: Reconciling relative sea level model predictions for the US East coast with geological constraints. *Geophys. J. Int.* **2015**, *201*, 1156–1181. [CrossRef]
21. Roy, K.; Peltier, W.R. Space-geodetic and water level gauge constraints on continental uplift and tilting over North America: Regional convergence of the ICE-6G_C (VM5a/VM6) models. *Geophys. J. Int.* **2017**, *210*, 1115–1142. [CrossRef]
22. Lambeck, K.; Purcell, A. Sea-level change in the Mediterranean Sea since the LGM: Model predictions for tectonically stable areas. *Quater. Sci. Rev.* **2005**, *24*, 1969–1988. [CrossRef]
23. Roy, K.; Peltier, W.R. Relative sea level in the Western Mediterranean basin: A regional test of the ICE-7G_NA (VM7) model and a constraint on Late Holocene Antarctic deglaciation. *Quat. Sci. Rev.* **2018**, *183*, 76–87. [CrossRef]
24. Melini, D.; Spada, G. Some remarks on glacial isostatic adjustment modelling uncertainties. *J. Geophys. Int.* **2019**, *218*, 401–413. [CrossRef]
25. Cardello, G.; Antonioli, F.; Barreca, G.; Monaco, C. First comparison of instrumental European Ground Motion Service by Copernicus data with short and long term geological vertical movements for the Italian coasts. In Proceedings of the XXI INQUA Congress, From Natural Processes to Geohazards Session 176: Tectonic and Climate-Driven Landscape Evolution a Never-Ending Challenge for Modern, Roma, Italy, 14–20 July 2023; Volume #4107.
26. Antonioli, F.; Ferranti, L.; Stocchi, P.; Deiana, G.; Lo Presti, V.; Furlani, S.; Marino, C.; Orru, P.; Scicchitano, G.; Trainito, E.; et al. Morphometry and elevation of the last interglacial tidal notches in tectonically stable coasts of the Mediterranean Sea. *Earth-Sci. Rev.* **2018**, *185*, 600–623.
27. Howes, D.; Dawson, A.; Smith, D. Late Holocene coastal tectonics at Falasarna_western_Crete a sedimentary sedimentary. *Geol. Soc. Lond. Spec. Publ.* **1998**, *146*, 343–352. [CrossRef]
28. Anzidei, M.; Antonioli, F.; Benini, A.; Gervasi, A.; Guerra, I. Evidence of vertical tectonic uplift at Briatico (Calabria, Italy) inferred from Roman age maritime archaeological indicators. *Quat. Int.* **2012**, *288*, 158–167. [CrossRef]
29. Faccenna, C.; Becker, T.; Auer, L.; Billi, A.; Boschi, L.; Brun, J.P.; Capitanio, F.; Funiciello, F.; Horvàth, F.; Jolivet, L.; et al. Mantle dynamics in the Mediterranean. *Rev. Geophys.* **2014**, *52*, 283–332. [CrossRef]
30. Oikonomou, P.; Karkani, A.; Evelpidou, N.; Kampolis, I.; Spada, G. The Fish Tanks of the Mediterranean Sea. *Quaternary* **2023**, *6*, 24. [CrossRef]